

1 **Measurement of jet yield and acoplanarity using**  
2 **semi-inclusive  $\gamma_{\text{dir}}+\text{jet}$  and  $\pi^0+\text{jet}$  distributions in  $p+p$**   
3 **and central Au+Au collisions at  $\sqrt{s_{\text{NN}}} = 200$  GeV by**  
4 **STAR**

---

5 **Derek Anderson (for the STAR Collaboration)<sup>a,\*</sup>**

6 <sup>a</sup>*Cyclotron Institute, Texas A&M University,*  
7 *TAMU 3366, College Station, TX 77843*

8 *E-mail: [derekwigam9@tamu.edu](mailto:derekwigam9@tamu.edu)*

9 The STAR collaboration presents measurements of semi-inclusive distributions of charged jets recoiling from high transverse energy ( $E_T$ ) direct photon and  $\pi^0$  triggers in  $p+p$  and central Au+Au collisions at  $\sqrt{s_{\text{NN}}} = 200$  GeV. Jets are reconstructed from charged particles using the anti- $k_T$  algorithm with jet resolution parameters  $R = 0.2$  and  $0.5$ . The large uncorrelated background in central Au+Au collisions is corrected using a mixed-event technique. This enables a jet measurement extending to low transverse momentum and large  $R$  with well-controlled systematic uncertainties. We present measurements of the jet  $R$  dependence of suppression, intra-jet broadening, and acoplanarity of  $\pi^0+\text{jet}$  and  $\gamma_{\text{dir}}+\text{jet}$  for trigger  $E_T$  between 9 – 20 GeV.

*41st International Conference on High Energy physics - ICHEP2022*  
*6-13 July, 2022*  
*Bologna, Italy*

---

\*Speaker

## 10 **1. Introduction**

11 Heavy-ion collisions at RHIC and the LHC produce a medium of deconfined partons, the  
12 Quark-Gluon Plasma (QGP) [1]. Hard (large momentum transfer,  $Q^2$ ) interactions of quarks and  
13 gluons in such collisions generate energetic scattered partons which propagate through the medium  
14 and interact with it. Consequently, the parton showers are modified, a phenomenon known as jet  
15 quenching [2]. Jet quenching manifests in several observable effects: transport of energy outside  
16 of the reconstructed jet cone, modification of the jet substructure, and enhanced acoplanarity  
17 ( $\Delta\phi = \phi_{\text{trig}} - \phi_{\text{jet}}$ ) [4]. While the  $\Delta\phi$  distribution has a finite width in vacuum due to Sudakov  
18 radiation [3], the presence of a medium may further broaden it due to mechanisms such as multiple  
19 in-medium soft scatterings [4], the hard scattering of a parton off QGP quasi-particles [5], and  
20 medium response [6].

21 In these proceedings, the STAR collaboration reports measurements of the semi-inclusive yields  
22 of jets recoiling from direct photons ( $\gamma_{\text{dir}}$ ) and  $\pi^0$ , together with their acoplanarity distributions  
23 in  $p+p$  and central Au+Au collisions at  $\sqrt{s_{\text{NN}}} = 200$  GeV. Simultaneous measurements of these  
24 different observables in the same analysis promise a discriminating and multi-messenger approach  
25 to the study of jet quenching.

26 Since  $\gamma_{\text{dir}}$  are color neutral, they do not interact strongly with the QGP; their measured energy  
27 thus reflects the  $Q^2$  of the hard interaction and provides a constraint on the initial energy of the  
28 recoiling jet. Hence, the measurement of jets coincident with a  $\gamma_{\text{dir}}$  ( $\gamma_{\text{dir+jet}}$ ) provides a valuable  
29 tool for quantifying the effects of jet quenching [7]. In addition, comparison with jets coincident  
30 with  $\pi^0$  ( $\pi^0$ +jet) may elucidate the color factor and path length dependence of medium-induced  
31 energy loss, due to differences between the recoil jet populations of the two triggers in their relative  
32 quark/gluon fraction and their mean path length [8].

33 STAR has previously reported the yield suppression of charged hadrons coincident with  $\pi^0$   
34 and  $\gamma_{\text{dir}}$  triggers [9]. Additionally, STAR has measured the yield of reconstructed charged-particle  
35 jets coincident with charged hadron triggers ( $h^\pm$ +jet) using a semi-inclusive approach [10]. In this  
36 approach, the large uncorrelated jet background in heavy-ion collisions is corrected with a Mixed  
37 Event (ME) technique, enabling the measurement of reconstructed jets at low transverse momentum  
38 ( $p_{\text{T}}$ ) and large resolution parameter. In the current analysis, we combine the  $\gamma_{\text{dir}}/\pi^0$  identification  
39 of [9] with the semi-inclusive and ME approach of [10] to measure the semi-inclusive  $\gamma_{\text{dir+jet}}$  and  
40  $\pi^0$ +jet yields in  $p+p$  and central Au+Au collisions.

## 41 **2. Analysis**

42 Two STAR datasets of  $\sqrt{s_{\text{NN}}} = 200$  GeV collisions are analyzed: a  $10 \text{ nb}^{-1}$  sample of Au+Au  
43 collisions recorded in 2014, and a  $23 \text{ pb}^{-1}$  sample of  $p+p$  collisions recorded in 2009. Both  
44 were recorded using an online high tower trigger, a calorimeter tower above a certain threshold in  
45 transverse energy. Two STAR subsystems are used: the Time Projection Chamber (TPC) [11], which  
46 provides charged-particle tracks for jet reconstruction, and the Barrel Electromagnetic Calorimeter  
47 (BEMC) [12], which is used to identify  $\pi^0$  and  $\gamma_{\text{dir}}$  triggers.

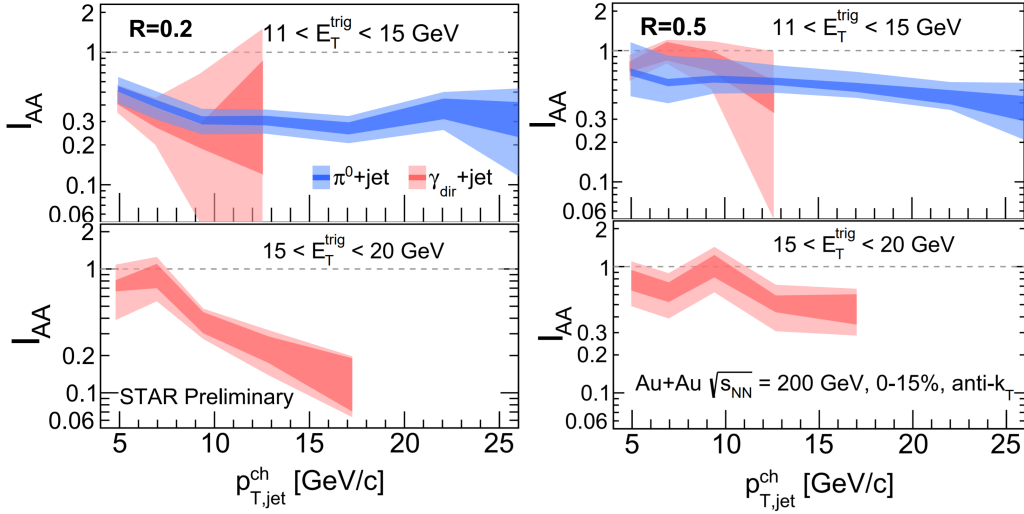


**Figure 1:**  $I_{AA}$  for  $\pi^0+\text{jet}$  (blue) and  $\gamma_{\text{dir}}+\text{jet}$  (red). Dark bands indicate statistical errors, and light bands indicate systematic uncertainties.

48 Discrimination of  $\pi^0$  and  $\gamma_{\text{dir}}$  candidates in the BEMC is carried out using the Transverse  
 49 Shower Profile (TSP) method [9, 13]. Based on the TSP, the data are separated into two samples:  
 50 a nearly pure sample of identified  $\pi^0$ , and a sample with an enhanced fraction of  $\gamma_{\text{dir}}$  ( $\gamma_{\text{rich}}$ ).

51 Triggers are selected offline which have a transverse energy ( $E_T$ ) of  $E_T^{\text{trig}} = 9 - 20$  GeV and  
 52 a pseudorapidity of  $|\eta^{\text{trig}}| < 0.9$ . The purity of the  $\gamma_{\text{rich}}$  sample, the percentage of  $\gamma_{\text{rich}}$  that are  
 53 actually  $\gamma_{\text{dir}}$ , is determined via a data driven method [9, 13]. The  $\gamma_{\text{dir}}+\text{jet}$  distribution is then  
 54 determined from the  $\gamma_{\text{rich}}$  sample via a statistical subtraction, which removes contamination due to  
 55 hadronic decays and fragmentation photons to the extent that their near-side azimuthal correlations  
 56 are identical to those of the identified  $\pi^0$  [9, 13].

57 Jets are reconstructed from the TPC tracks using the anti- $k_T$  algorithm [14, 15] for two resolution  
 58 parameters,  $R = 0.2$  and  $0.5$ . Reconstructed jets are subjected to the same fiducial cuts as in [10].

59 In Au+Au collisions, there is a substantial background yield of jet candidates which are not  
 60 correlated with the trigger. This background yield is removed using the ME technique described in  
 61 [10]. The uncorrelated jet yield is small in  $p+p$  collisions, and so no correction for it is applied.  
 62 The residual jet transverse momentum ( $p_T$ ) smearing is corrected in two steps [10]: first, jets are  
 63 corrected for an event-wise energy pedestal, and then residual fluctuations caused by detector effects  
 64 ( $p+p$  and Au+Au collisions) and the heavy-ion background (Au+Au collisions only) are corrected  
 65 using regularized unfolding. We use  $p_{T,\text{jet}}^{\text{reco,ch}}$  (where the superscript “ch” denotes “charged jets”) to  
 66 refer to the jet  $p_T$  after the event-wise pedestal correction, and  $p_{T,\text{jet}}^{\text{ch}}$  to the jet  $p_T$  after unfolding.

67 The two-dimensional acoplanarity distributions must also be unfolded for both  $p_{T,\text{jet}}^{\text{reco,ch}}$  and  $\Delta\phi$   
 68 fluctuations. Note that the  $\Delta\phi$  distributions shown here have been unfolded for  $p_{T,\text{jet}}^{\text{reco,ch}}$  fluctuations  
 69 only. We estimate that the  $\Delta\phi$  smearing effects are small.

### 70 3. Results

71 Jet distributions are reported in two ways: the two-dimensional measurement of  $\Delta\phi$  vs.  $p_{T,\text{jet}}^{\text{ch}}$ ,  
 72 and the one-dimensional measurement of  $p_{T,\text{jet}}^{\text{ch}}$  for recoil jets, which satisfy  $|\Delta\phi - \pi| < \pi/4$ . The  
 73 recoil jet  $p_{T,\text{jet}}^{\text{ch}}$  distributions in central Au+Au and  $p+p$  collisions are compared against PYTHIA-8  
 74 with the MONASH tune [16]. The PYTHIA-8 distributions are smeared to account for the trigger  
 75 energy resolution. We report two different ratios of the trigger-normalized recoil jet yields:  $I_{AA}$ , the  
 76 ratio of the semi-inclusive yield of recoil jets in Au+Au over that in  $p+p$  for fixed  $R$ ; and  $\mathfrak{R}^{0.2/0.5}$ ,  
 77 the ratio of the semi-inclusive yield for  $R = 0.2$  jets relative to that for  $R = 0.5$  jets, for fixed  
 78 collision system.

79 Figure 1 shows  $I_{AA}$  for  $E_T^{\text{trig}} = 11 - 15, 15 - 20$  GeV  $\pi^0$  and  $\gamma_{\text{dir}}$  triggers. The recoil jet  
 80 yield for  $R = 0.2$  is systematically more suppressed than that for  $R = 0.5$ . In addition, the value  
 81 of  $I_{AA}$  is observed to be consistent within uncertainties between  $\pi^0$  and  $\gamma_{\text{dir}}$  for both values of  $R$ ,  
 82 despite differences in the recoil jet quark/gluon fraction and mean path length. Note, however, that  
 83 the  $\gamma_{\text{dir}}+\text{jet}$   $p_{T,\text{jet}}^{\text{ch}}$  spectrum is steeper, so a similar magnitude of yield suppression corresponds to  
 84 smaller medium-induced out-of-cone energy loss.

85 Figure 2 shows the  $\mathfrak{R}^{0.2/0.5}$  for  $E_T^{\text{trig}} = 11 -$   
 86 15 GeV  $\pi^0$  (upper panel) and  $E_T^{\text{trig}} = 15 - 20$   
 87 GeV  $\gamma_{\text{dir}}$  (lower panel). We see that  $\mathfrak{R}^{0.2/0.5}$   
 88 for  $p+p$  is less than unity and that PYTHIA-8  
 89 reproduces the ratio well. However, the value  
 90 of  $\mathfrak{R}^{0.2/0.5}$  for central Au+Au is significantly  
 91 lower than that for  $p+p$  and PYTHIA-8.

92 Figures 1 and 2 show a clear observation  
 93 of significant medium-induced intra-jet broad-  
 94 ening in central Au+Au collisions at RHIC.

95 Figure 3a shows the corrected  $\Delta\phi$  correla-  
 96 tions in  $p+p$  collisions between  $E_T^{\text{trig}} = 9 - 11$   
 97 GeV  $\pi^0$  triggers and  $R = 0.5$  jets (boxes). These  
 98 distributions are reproduced well by PYTHIA-8  
 99 (dotted lines) for all three ranges of  $p_{T,\text{jet}}^{\text{ch}}$  (5–10,  
 100 10–15, and 15–20 GeV/c).

101 Figure 3b then shows the corrected  $\Delta\phi$  cor-  
 102 relations in Au+Au collisions between  $E_T^{\text{trig}} =$   
 103 11–15 GeV  $\pi^0$  and  $\gamma_{\text{dir}}$  triggers and recoil jets of  $R = 0.5$  and  $p_{T,\text{jet}}^{\text{ch}} = 10 - 15$  GeV/c. The dashed  
 104 lines are the corresponding distributions from PYTHIA-8, that is validated in the left panel. We ob-  
 105 serve a marked enhancement in yield at wide angles (small  $\Delta\phi$ ) in central Au+Au collisions relative  
 106 to vacuum fragmentation. This is the first observation of significant medium-induced modification  
 107 of  $\pi^0+\text{jet}$  and  $\gamma_{\text{dir}}+\text{jet}$  acoplanarity at low  $p_{T,\text{jet}}^{\text{ch}}$  in central Au+Au collisions at RHIC.

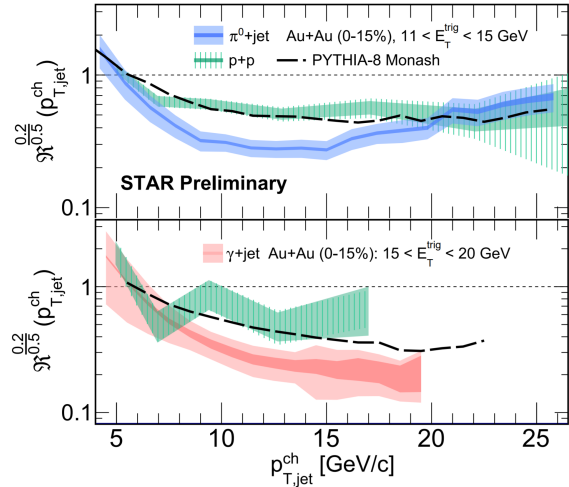


**Figure 2:**  $\mathfrak{R}^{0.2/0.5}$  for  $\pi^0$  (upper panel) and  $\gamma_{\text{dir}}$  (lower panel) triggers from  $p+p$  (green), Au+Au (blue and red), and PYTHIA-8 (black dashed lines).

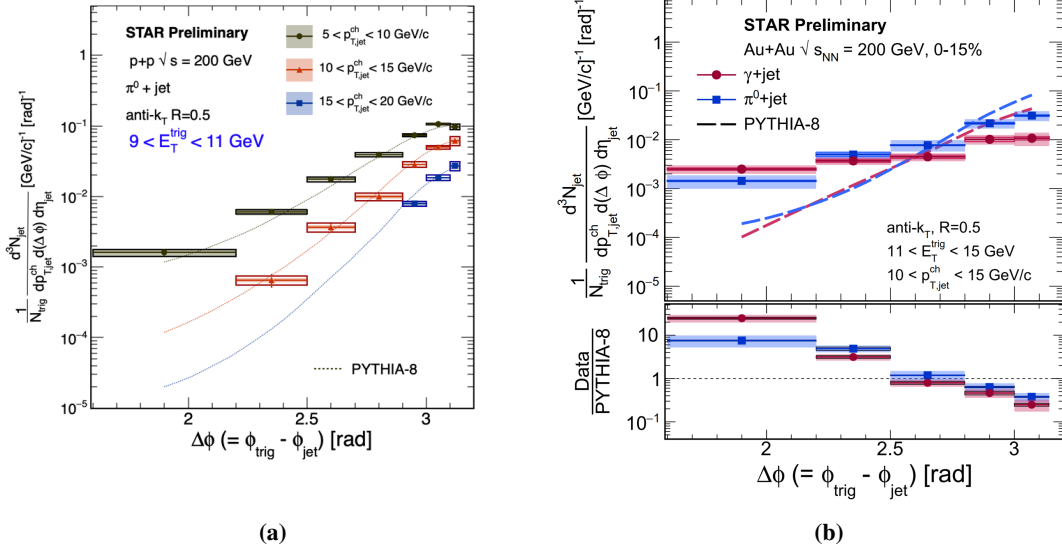


**Figure 3:** Corrected  $R = 0.5$   $\Delta\phi$  distributions in  $p+p$  (a) and Au+Au (b) collisions for  $\pi^0$  ( $p+p$  and Au+Au) and  $\gamma_{\text{dir}}$  (Au+Au only) triggers. Vertical lines around data points indicate statistical errors, and filled and open boxes indicate uncorrelated and correlated systematic uncertainties respectively (note that the statistical errors are smaller than the marker size for the Au+Au data points). Dotted and dashed lines are PYTHIA-8.

## 108 4. Summary

109 STAR has measured the  $R$  dependence of recoil jet yield, and acoplanarity using the semi-  
 110 inclusive distributions of charged-particle jets recoiling from  $\pi^0$  and  $\gamma_{\text{dir}}$  triggers in central Au+Au  
 111 and  $p+p$  collisions at  $\sqrt{s_{\text{NN}}} = 200 \text{ GeV}$ . Model calculations based on the PYTHIA-8 event generator  
 112 are found to be consistent with the measurements in  $p+p$  collisions.

113 We have reported both the recoil yield in a fixed angular window as a function of  $p_{\text{T,jet}}^{\text{ch}}$ ,  
 114 and the distribution of acoplanarity at fixed  $p_{\text{T,jet}}^{\text{ch}}$ . We observe marked medium-induced intra-jet  
 115 broadening. We also observe clear medium-induced acoplanarity at low jet  $p_{\text{T,jet}}^{\text{ch}}$ , which may arise  
 116 from in-medium jet scattering or from the contribution of medium response to the jet signal. To  
 117 further investigate the medium-induced acoplanarity and disentangle the underlying mechanisms,  
 118 it will be essential to extend the kinematic range of this measurement in heavy-ion collisions and  
 119 compare against theoretical calculations.

## 120 Acknowledgements

121 This work is funded in part by the United States Department of Energy under grant number  
 122 DE-SC0015636.

## 123 References

- 124 [1] W. Busza, K. Rajagopal, and W. van der Schee, *Ann. Rev. Nucl. Part. Sci.* **68**, 339 (2018)  
 125 [2] L. Cunqueiro and A. M. Sickles, (2021) arXiv:2110.14490 [nucl-ex]

- 126 [3] P. Sun, C.-P. Yuan, and F. Yuan, Phys. Rev. D **92**, 094007 (2015)
- 127 [4] A. Mueller *et al.*, Phys. Lett. B **763**, 208 (2016)
- 128 [5] F. D'Eramo, M. Lekaveckas, H. Liu, and K. Rajagopal, J. High Energy Phys. **2013**, 031 (2013)
- 129 [6] G. Milhano, U. A. Wiedemann, and K. C. Zapp, Phys. Lett. B **779**, 409 (2018)
- 130 [7] X.-N. Wang, Z. Huang, and I. Sarcevic, Phys. Rev. Lett. **77**, 231 (1996)
- 131 [8] T. Renk, PRC **88**, 054902 (2013)
- 132 [9] L. Adamczyk *et al.*, Phys. Lett. B **760**, 689(2016)
- 133 [10] L. Adamczyk *et al.*, Phys. Rev. C **96**, 024905 (2017)
- 134 [11] M. Anderson *et al.*, Nucl. Instrum. Methods Phys. Res., Sect. A **499**, 659 (2003)
- 135 [12] M. Beddo *et al.*, Nucl. Instrum. Methods Phys. Res., Sect. A **499**, 725 (2003)
- 136 [13] B. I. Abelev *et al.*, Phys. Rev. C **82**, 034909 (2010)
- 137 [14] M. Cacciari, G. P. Salam, and G. Soyez, J. High Energy Phys. **2008**, 063 (2008)
- 138 [15] M. Cacciari, G. P. Salam, and G. Soyez, Euro. Phys. J. C **72**, 1896 (2012)
- 139 [16] T. Sjöstrand, S. Mrenna, and P. Z. Skands, Comput. Phys. Commun. **178**, 852 (2008)